Advanced Physical Research
Vol.6, No.3, 2024, pp.166-174
https://doi.org/10.62476/apr63166

IDENTIFYING THE FINE STRUCTURE OF THE EXPERIMENTALLY OBSERVED PEAK FOR ^{254}No AT 2.5 MeV

H. Quliyev[1,2*], E. Guliyev[3], A.A. Kuliev[2]

[1]Department of Economic and Technological Sciences, International Magistrate and Doctorate Center, Azerbaijan State University of Economics (UNEC), Baku, Azerbaijan
[2]National Aviation Academy, Baku, Azerbaijan
[3]State Agency for Regulation of Nuclear and Radiological Activity, Ministry of Emergency Situations, Baku, Azerbaijan

Abstract. Thus far, the low-lying dipole response has been observed throughout the deformed nuclear chart, with the exception of the transfermium region. In addition, the spectroscopic energy region of the ^{254}No nucleus has recently been investigated and a broad peak at ≈ 2.5 MeV has been observed. This study, for the first time, explains the fine structure of this experimentally observed broad peak by predicting it through the QRPA framework. More specifically, the calculations revealed the experimentally observed peak comprises at least six dipole excitations.

Keywords: *Electric and magnetic dipole excitations, transfermium nuclide, ^{254}No, QRPA, scissor mode.*

Corresponding Author: *Huseynqulu Quliyev, Department of Economic and Technological Sciences, International Magistrate and Doctorate Center, Azerbaijan State University of Economics (UNEC), Baku, Azerbaijan, Tel.: +994558370174, e-mail: huseynqulu@yahoo.com*

Received: *18 June 2024;* ***Accepted:*** *3 September 2024;* ***Published:*** *16 October 2024.*

1. Introduction

The scissors mode has been investigated across a broad spectrum of nuclei, ranging from less-deformed transitional and γ-soft nuclei to deformed nuclei within the rare-earth and actinide regions, with these studies taking both experimental (Margraf *et al*., 1990; 1995; Herzberg *et al*., 1993; Friedrichs *et al*., 1994; Von Brentano *et al*., 1996; Reif *et al*., 1997; Schwengner *et al*., 1997; Fransen *et al*., 1999; 2003; Pietralla *et al*., 1999; Linnemann *et al*., 2003; Von Garrel *et al*., 2006; Garrote *et al*., 2022) and theoretical (Hamamoto & Åberg 1986; Nojarov & Faessler 1990; Kuliev *et al*., 2000; 2004; 2010; Guliyev *et al*., 2001; 2006; 2022; Heyde *et al*., 2010; Zenginerler *et al*., 2013; Tabar *et al*., 2022) approaches. Recent studies of the scissors mode have tended to focus on super heavy nuclei, however (Garrote *et al*., 2022). In this context, the excitations of the super heavy ^{254}No nucleus produced in the ^{208}Pb(^{48}Ca, 2nγ)^{254}No reaction, where the spectrum of γ rays are below the 4 MeV region, were measured (Garrote *et al*., 2022). By measuring the linear polarization properties of the emitted γ-rays, the experimental study observed that dipole transitions directly predicted a magnetic dipole peak at around the

How to cite (APA):
Quliyev H., Guliyev, E. & Kuliev, A.A. (2024). Identifying the fine structure of the experimentally observed peak for ^{254}No at 2.5 MeV. *Advanced Physical Research, 6*(3), 166-174 https://doi.org/10.62476/apr63166

2.4-2.6 MeV range, but it was impossible to detect its fine structure. Although the observation provides very important information about the scissors mode for transfermium nuclei, our knowledge is confined due to the lack of information about the fine structure of the observed peak.

Other theoretical and experimental works in the 2-4 MeV energy region have shown that *E1* states are also present in the spectroscopic region (Iudice & Richter 1989; 1993; Kneissl *et al*., 1996; 2006; Kuliev *et al*., 2000), so it is necessary to investigate the fine structure of the observed peak.

Thus, for the first time, the fine structure of the experimentally observed peak at ≈ 2.5 MeV for the ^{254}No nucleus is explained in this study, with the rotational Invariant (RI-), Translation and Galileo Invariant (TGI-) Quasiparticle Random Phase Approximation (QRPA) framework being used to achieve this. Furthermore, to obtain detailed information about this observed peak, we investigated the electric and magnetic dipole excitations in the same range.

The invariance QRPA model applied in this study has demonstrated its effectiveness at describing *E1* and *M1* transitions in deformed nuclei (Kuliev *et al*., 2010; Guliyev *et al*., 2020; Quliyev *et al*., 2021; 2023; Tabar *et al*., 2022). In particular, our recent research suggests that the invariance QRPA model is also an effective tool for investigating dipole excitations, such that it is on a par with the latest QRPA models that have been applied to investigate dipole excitations (Guliyev *et al*., 2023).

2. Theory

The Hamiltonian which produces magnetic dipole states of deformed nuclei, single particle Hamiltonian (H_{sqp}), spin-spin forces ($V^{\sigma\tau}$) and isoscaler (h_0) and isovector (h_1) restoration interactions is written as follows (Kuliev *et al*., 2000):

$$H = H_{sqp} + h_0 + h_1 + V_{\sigma\tau} \ , \tag{1}$$

$$H_{sqp} = \sum_{qq'} \varepsilon_s(\tau) B_{qq'}(\tau) \ , \tag{2}$$

$$V_{\sigma\tau} = \frac{1}{2}\chi_{\sigma\tau} \sum_{i\neq j} \vec{\sigma}_i \vec{\sigma}_j \vec{\tau}_i \ \vec{\tau}_j \ , \tag{3}$$

$$h_0 = -\frac{1}{2\gamma_0} \sum_{\mu} [H_{sqp} - V_1, J_\mu]^+ [H_{sqp} - V_1, J_\mu] \ , \tag{4}$$

$$h_1 = -\frac{1}{2\gamma_1} \sum_{\mu} [V_1, J_\mu]^+ [V_1, J_\mu], \tag{5}$$

where σ and τ are Pauli matrices representing spin and isotopic spin, respectively.

The model Hamiltonian, which produces 1^- states in deformed nuclei, includes H_{sqp} the single-quasiparticle Hamiltonian (Equation 2), isovector part of dipole-dipole interaction (W_1)and the h_0 and h_Δ restoration interactions for broken translational and Galilean symmetries is (Guliyev *et al*., 2002; Kuliev *et al*., 2010):

$$H = H_{sqp} + h_0 + h_\Delta + W_1 \, , \tag{6}$$

$$h_0 = -\frac{1}{2\gamma} \sum_{\mu} [H_{sqp}, P_\mu]^+ [H_{sqp}, P_\mu] \ , \tag{7}$$

$$h_{\Delta} = -\frac{1}{2\beta}\sum_{\mu}[U_{\Delta}, P_{\mu}]^{+}[U_{\Delta}, P_{\mu}], \tag{8}$$

$$W_1 = \frac{3}{2\pi}\chi_1\left(\frac{NZ}{A}\right)^2(\vec{R}_n - \vec{R}_p)^2. \tag{9}$$

Using the well-known procedure of QRPA, the eigenvalues and eigenfunctions of the Hamiltonian are found by solving the following equation of motion for the *E1* and *M1* states.

$$\left[H, Q_i^{+}\right] = \omega_i Q_i^{+} \ . \tag{10}$$

The reduced probabilities of *M1* and *E1* transitions for even-even deformed nuclei can be obtained using the mathematical expression within the framework of QRPA using the following

$$B\left(E1, 0 \to 1^{-}K\right) = \left(1 + \delta_{K,1}\right)\frac{1}{Y(\omega_i)}\left|\left(e_{eff}^{p} M_p + e_{eff}^{n} M_n\right)\right|^2, \tag{11}$$

$$B(M1, 0 \to 1^{+}K) = \frac{3}{4\pi}\left|R_p^j(\omega_i) + \sum_{\tau}(g_s^{\tau} - g_l^{\tau})R_{\tau}(\omega_i)\right|^2 \mu_N^2 \ . \tag{12}$$

Radiation width of *E1* and *M1* excitations are given as follows

$$\Gamma(M1) = 3{,}86\omega_i^3 \ \mathrm{B(M1)\ meV}, \tag{13}$$

$$\Gamma(E1) = 3{,}349\omega_i^3 \ \mathrm{B}(E1)\ \mathrm{meV}, \tag{14}$$

where the excitation energy ω_i is in MeV, B(*M1*) in $\mu_N^2 = (e\hbar/2m_nc)^2$ and B(*E1*) in $10^{-3}e^2fm^2$. More detailed information about the expressions given in Equations (1-14) and the abbreviations in these expressions are given in detail in our previous studies. For more detailed information on the RI-QRPA and TGI-QRPA models we used for *M1* and *E1* transitions, respectively (Kuliev *et al*., 2000; Quliyev *et al*., 2021; 2023; Guliyev *et al*., 2023).

3. Results and Discussion

The QRPA calculations were performed with the single particle energies and wave functions that were obtained from the axially symmetric Woods–Saxon potential (Dudek & Werner, 1978), which used the deformation parameters taken from Garrote et al. (2022). The total number of two-quasiparticle magnetic and electric states, which have maximum energies up to 40 MeV, was 2,227 (827 for K=0 and 1400 for K=1) and 1,869 (891 for K=0 and 968 for K=1), respectively. The pairing between the quasiparticles was calculated using the conventional BCS equations that can be found in Soloviev (1976). The chemical potentials were calculated according to Soloviev's method (1976), while the theoretical parameters are presented in Table 1.

Table 1. Pairing Δ_n (Δ_p) and chemical λ_n (λ_p) parameters, δ_2 and β_2 values

Nucleus	β_2	δ_2	Δ_n [MeV]	Δ_p [MeV]	λ_n [MeV]	λ_p [MeV]
$^{254}_{108}No_{146}$	0.27	0.24	0.63	0.72	-7.000	-3.437

For the calculations, the isovector dipole-dipole interaction constant (χ_1) for *E1* excitations and the isovector spin-isospin interaction constant ($\chi_{\sigma\tau}$) for *M1* excitations were set at $\chi_1=400/A^{5/3}$ MeV·fm^{-2} and $\chi_{\sigma\tau}=25/A$ MeV, respectively. These values have been found to be successful for explaining the scissors mode, giant dipole resonance (GDR) and pygmy dipole resonance (PDR) calculations for actinide nuclei (Kuliev *et al*., 2010; Tabar *et al*., 2021).

The calculations predict the number of electric and magnetic dipole excitations within the spectroscopic energy region, with both of these playing a significant role in forming the dipole structure of the spectroscopic region. The calculations predicted 31 magnetic dipole excitations, of which 24 were 1^+1 and 7 were 1^+0. The total B(*M1*) strength of the 1^+1 levels was 7.543 μ_N^2, whereas the total B(*M1*) strength of the 1^+0 levels was 0.790 μ_N^2. The calculation for the *E1* transition predicted 37 1^- states with $\Sigma B(E1)=48.722\cdot10^{-3}e^2fm^2$, where 21 of them were 1^-1 and 16 of them were 1^-0 states with $\Sigma B(E1)=38.592\cdot10^{-3}3e^2fm^2$ and $\Sigma B(E1)=10.130\cdot10^{-3}e^2fm^2$.

The dipole excitation strength distribution has been experimentally investigated, and this study observed one well-pronounced dipole excitation at around 2.5 MeV. In addition, by measuring the polarization asymmetry, an *M1* character was directly identified (Garrote *et al*., 2022) (See top side of Figure 1). Despite the experiment performing linear polarization analysis and the presence of *E1* states being detected, no *E1* spectrum was obtained for this region. The experimental points below 500 keV correspond to pure *E*2 transitions in the ground-state band. As can be seen, despite theoretically predicting several excitations below 2.4 MeV, no excitations were experimentally observed in this region. Therefore, in this study, through QRPA calculations, we attempt to explain the structure of the observed broad peak at 2.5 MeV (lower part of Figure 1). Taking into account its large structure and length in the experiment, the study confirmed that this peak is formed by a large group of discrete transitions. Thus, the theoretical calculations in this present study focus on investigating the fine structure of the peak at ≈ 2.5 MeV.

As can be seen from Figure 1, the peak around 2.5 MeV was experimentally observed with error bars between 2.4 and 2.6 MeV (Garrote *et al*., 2022), so to obtain detailed information about this observed peak, we here investigated the electric and magnetic dipole excitations within the same range.

As the units of *E1* and *M1* excitation differ for their transition strengths, we presented them in terms of the ground state radiation width. The results of the calculations are presented in Table 2.

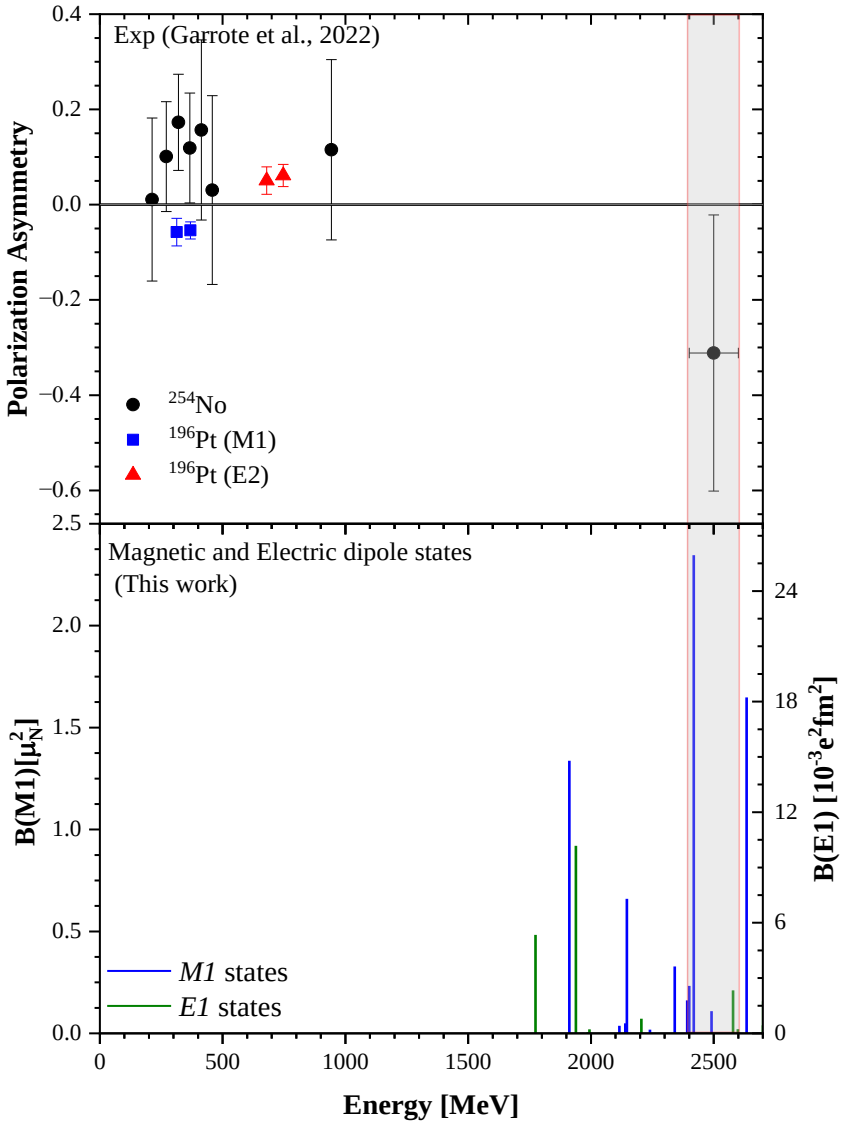

Figure 1. Comparison of the theoretical *M1* and *E1* dipole spectrums with experimental polarization asymmetry data in the region below 2500 keV for the ^{254}No nuclide

Table 2. The dipole strengths and radiation widths of dipole excitations in the 2.4–2.64 MeV region for the ^{254}No nuclide

M1				*E1*			
Branch	ω_i [MeV]	B(*M1*) [μ_N^2]	Γ(*M1*) [meV]	Branch	ω_i [MeV]	B(*E1*) [$10^{-3}e^2fm^2$]	Γ(*E1*) [meV]
K=1	2.400	0.233	12.4	K=1	2.579	2.335	2.2
K=1	2.419	2.346	128	K=0	2.598	0.223	1.4
K=1	2.491	0.109	6.52				
K=1	2.634	1.648	116				

As shown in our calculations, there are four *M1* (K=1) and two *E1* (K=1) excitations with total summed strengths of B(*M1*)=4.336μ_N^2 and B(*E1*)=0.597·10^{-3}e^{2}fm^2, respectively, at the energy range between 2.4 and 2.64 MeV. Two of the predicted *M1* excitations are well pronounced with transition strengths of 2.346 and 1.648μ_N^2. As the excitation at 2.634 MeV is very close to the experimentally observed peak, we included it here in our discussion. We can therefore say that the experimentally observed peak at 2.5 MeV comprises at list six excitations, with two of them being well-pronounced magnetic dipole excitations that belong to the scissors mode. Based on our calculations, 98.65% of the dipole excitations in the 2.4–2.64 MeV region have an *M1* character, so we can conclude that the experimentally observed peak mainly comprises magnetic dipole excitations. We would also like to point out that when we compare our theoretical predictions with the experimental polarization analysis, the *M1* state determined by the experimental polarization analysis at 2.5(1) MeV is probably the magnetic dipole excitations predicted here with transition strength B(*M1*)=2.346μ_N^2 at 2.419 MeV energy.

Figure 2 shows the *B(M1)* strengths obtained in this work and the experimental results estimated through the simulations (Garrote *et al*., 2022).

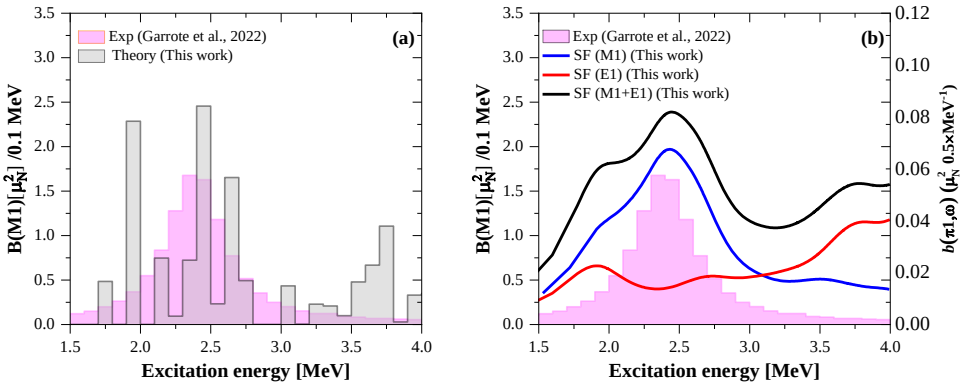

Figure 2. Distribution of the calculated magnetic and electric dipole excitations within the 1.5–4 MeV energy region together with the experimentally estimated results from Garrote et al. (2022)

In this present investigation, the B(πl) strength distributions for ^{254}No in the 1.5–4 MeV range were computed and juxtaposed with the experimental findings as well. To align with the histogram format of the simulation data from the experimental inquiry (Garrote *et al*., 2022), our theoretical outcomes were also presented through a histogram distribution in 100 keV steps, as shown in Figure 2a. Thus, to facilitate comparison with the experimental data, the theoretical probabilities for the *E1* and *M1* transitions were computed in 100 keV intervals in line with the experimental methodology. On comparing our theoretical results with the experimental data, it is clear that their distributions are compatible, especially for their maximums, which are very close to each other (around 2.5 MeV). After 2.8 MeV, there is a clear decrease in the dipole spectrum. Figure 2b also compares the theoretical dipole strength function with the experimental histogram and the theoretical predictions agree with the experimental histogram distribution.

As can be seen in the case of the theoretical results, the summed *E1* and *M1* strengths are 48.722 10^{-3}e^{2}fm^2 and 8.333μ_N^2, respectively. While the units for the *E1* and *M1* transitions are different, we could convert between 10^{-3}e^{2}fm^2 and μ_N^2 units. With a conversion factor of 1μ_N^2=11.06·10^{-3}e^{2}fm^2, the total strength of the *E1* transitions (48.722·10^{-3}e^{2}fm^2) corresponds to 4.405μ_N^2. When considering the *M1* and *E1* strengths of 8.333μ_N^2 and 4.405μ_N^2, respectively, the summed *M1+E1* strength in the 1.5–4 MeV

region is $12.738\mu_N^2$. Our theoretical result agrees with the experimental data in terms of the experimental errors. Moreover, our theoretical value is very consistent with the sum-rule estimate of B(*M1*)=12.1(13) μ_N^2 that is cited in the experimental paper (Garrote *et al*., 2022). When comparing our theoretical *E1* and *M1* results, we can see how *E1* transitions contribute approximately 35%, but this contribution was treated as *M1* states in the experimental observation. The centroid energy of the *M1* states is 2.546 MeV, while the energy centroids of the K=0 and K=1 branches are 3.318 MeV and 2.465 MeV, respectively. The centroid energy value was calculated as being 2.861 MeV for the *E1* levels, while it was found to be 3.351 MeV for the 1^-1 levels and 2.733 MeV for the 1^-0 levels. When considering the dipole spectrum, the centroid energy for the *M1+E1* dipole states was calculated as being 2.655 MeV, which broadly agrees with the experimental prediction (≈2.5 MeV), at least within the experimental error range.

4. Conclusion

Using the QRPA approach, this study identified the fine structure of the experimentally observed broad peak in the 2.4-2.6 MeV range for the first time. Moreover, our calculations showed that this experimentally observed peak comprises at least six electric and magnetic dipole excitations, with two of them being well-pronounced magnetic dipole excitations. The results presented here therefore contribute to advancing our understanding of the nuclear structure in superheavy nuclei and provide valuable guidance for future experimental studies in the field of nuclear physics.

References

Dudek, J., Werner, T. (1978). New parameters of the deformed Woods-Saxon potential for A= 110-210 nuclei. *Journal of Physics G: Nuclear Physics*, *4*(10), 1543.

Fransen, C., Krischok, B., Beck, O., Besserer, J., Von Brentano, P., Eckert, T. & Zilges, A. (1999). Low-lying dipole excitations in the transitional nuclei ^{190,192}Os. *Physical Review C, 59*(4), 2264.

Fransen, C., Pietralla, N., Ammar, Z., Bandyopadhyay, D., Boukharouba, N., Von Brentano, P. & Yates, S.W. (2003). Comprehensive studies of low-spin collective excitations in ^{94}Mo. *Physical Review C, 67*(2), 024307.

Friedrichs, H., Häger, D., Von Brentano, P., Heil, R.D., Herzberg, R.D., Kneissl, U. & Zilges, A. (1994). Low-lying E1 and M1 strengths in the deformed nucleus ^{160}Gd. *Nuclear Physics A, 567*(2), 266-280.

Garrote, F.B., Lopez-Martens, A., Larsen, A.C., Deloncle, I., Péru, S., Zeiser, F. & Uusitalo, J. (2022). Experimental observation of the M1 scissors mode in ^{254}No. *Physics Letters B*, 834, 137479.

Guliyev, E., Ertuğral, F. & Kuliev, A.A. (2006). Low-lying magnetic dipole strength distribution in the γ-soft even-even $^{130-136}$Ba. *The European Physical Journal A-Hadrons and Nuclei*, 27, 313-320.

Guliyev, E., Kuliev, A.A., Von Neumann-Cosel, P. & Richter, A. (2002). Nature of the scissors mode in nuclei near shell closure: The tellurium isotope chain. *Physics Letters B*, 532, 173.

Guliyev, E., Kuliev, A.A., Von Neumann-Cosel, P. & Yavas, Ö. (2001). Magnetic dipole strength distribution and photon interaction cross sections in ^{140}Ce. *Nuclear Physics A*, 690, 255.

Guliyev, E., Quliyev, H. & Kuliev A.A. (2020). Pygmy dipole resonance in the well deformed even-even $^{152-162}$Gd. *Journal of Physics G: Nuclear and Particle Physics*, 47, 115107.

Guliyev, E., Quliyev, H. & Kuliev, A.A. (2022). Role of the quadrupole deformation in g-soft nuclei: the case of $^{124-134}$Xe. *Nuclear Physics A*, 1027, 122496.

Guliyev, E., Quliyev, H. & Kuliev, A.A. (2023). Effectiveness of the TGI-QRPA approach for studying the electric dipole response. *Physica Scripta*, 98, 125309.

Hamamoto, I., Åberg, S. (1986). Structure of low-lying $K^{\pi}= 1^{+}$ mode in a microscopic model. *Physica Scripta*, 34, 697.

Herzberg, R.D., Zilges, A., Von Brentano, P., Heil, R., Kneissl, U., Margraf, J., Pitz, H., Friedrichs, H., Lindenstruth, S. & Wesselborg, C. (1993). Investigation of low-lying dipole excitations in ^{182,184,186}W. *Nuclear Physics A*, 563, 445.

Heyde, K., Von Neumann-Cosel, P. & Richter, A. (2010). Magnetic dipole excitations in nuclei: Elementary modes of nucleonic motion. *Reviews of Modern Physics*, 82, 2365.

Iudice, N.L., Richter, A. (1989). Orbital magnetic dipole excitations in deformed nuclei and the scissors mode. *Physics Letters B*, 228, 291.

Iudice, N.L., Richter, A. (1993). Scissors mode and nuclear deformation. A phenomenological model independent analysis. *Physics Letters B*, 304, 193.

Kneissl, U., Pietralla, N. & Zilges, A. (2006). Low-lying dipole modes in vibrational nuclei studied by photon scattering. *Journal of Physics G: Nuclear and Particle Physics*, 32, R217.

Kneissl, U., Pitz, H. & Zilges, A. (1996). Investigation of nuclear structure by resonance fluorescence scattering. *Progress in Particle and Nuclear Physics*, 37, 349.

Kuliev, A., Faessler, A., Güner, M. & Rodin, V. (2004). Fully renormalized quasi-particle random phase approximation, spurious states and ground state correlations. *Journal of Physics G: Nuclear and Particle Physics*, 30, 1253.

Kuliev, A.A., Akkaya, R., Ilhan, M., Guliyev, E., Salamov, C. & Selvi, S. (2000). Rotational-invariant model of the states with $K^{\pi}= 1^{+}$ and their contribution to the scissors mode. *International Journal of Modern Physics E*, 9, 249.

Kuliev, A.A., Guliyev, E., Ertugral, F. & Özkan, S. (2010). The low-energy dipole structure of ^{232}Th, 236U and 238U actinide nuclei. *The European Physical Journal A*, 43, 313.

Linnemann, A., Von Brentano, P., Eberth, J., Enders, J., Fitzler, A., Fransen, C. & Wiedenhöver, I. (2003). Change of the dipole strength distributions between the neighbouring γ-soft nuclei ^{194}Pt and ^{196}Pt. *Physics Letters B*, *554*(1-2), 15-20.

Margraf, J., Degener, A., Friedrichs, H., Heil, R.D., Jung, A., Kneissl, U. & Zilges, A. (1990). Photoexcitation of low-lying dipole transitions in ^{236}U. *Physical review C*, *42*(2), 771.

Margraf, J., Eckert, T., Rittner, M., Bauske, I., Beck, O., Kneissl, U. & Friedrichs, H. (1995). Systematics of low-lying dipole strengths in odd and even Dy and Gd isotopes. *Physical Review C*, *52*(5), 2429.

Nojarov, R., Faessler, A. (1990). Low-collective scissors mode. *Zeitschrift für Physik A Atomic Nuclei*, *336*(2), 151-157.

Pietralla, N., Fransen, C., Belic, D., Von Brentano, P., Frießner, C., Kneissl, U. & Wiedenhöver, I. (1999). Transition rates between mixed symmetry states: First measurement in ^{94}Mo. *Physical Review Letters*, *83*(7), 1303.

Quliyev, H., Guliyev, E. & Kuliev, A.A. (2021). Electric dipole strength in the deformed ^{144,146,148,150,152,154}Nd nuclei. *Nuclear Physics A*, 1014, 122239.

Quliyev, H., Guliyev, E. & Kuliev, A.A. (2023). Dipole responses in γ−soft $^{124\text{-}134}$Xe in the spectroscopic energy region. *Journal of Physics G: Nuclear and Particle Physics*, 50, 025101.

Reif, J., Von Brentano, P., Eberth, J., Enders, J., Herzberg, R.D., Huxel, N. & Zilges, A. (1997). Resonant photon scattering on the semi-magic nucleus ^{89}Y up to 7 MeV. *Nuclear Physics A*, *620*(1), 1.

Schwengner, R., Winter, G., Schauer, W., Grinberg, M., Becker, F., Von Brentano, P. & Zilges, A. (1997). Two-phonon J=1 states in even-mass Te isotopes with A= 122–130. *Nuclear Physics A*, *620*(3), 277-295.

Soloviev, V.G. (1976). *Theory of Complex Nuclei*. Pergamon Press, New York, USA.

Tabar, E., Yakut, H., Hoşgör, G. & Kemah, E. (2022). Scissors mode and effects of the low-lying E1 excitations on the dipole distributions in ^{175}Lu. *Physica Scripta*, 97, 065303.

Tabar, E., Yakut, H., Kemah, E., Saygı, N.D., Hoşgör, G., Quliyev, H. & Kuliev, A.A. (2021). Systematics of electric dipole excitations for odd-mass $^{233-239}$U isotopes. *Nuclear Physics A*, 1008, 122138.

Von Brentano P., Eberth J., Enders J., Esser L., Herzberg R.-D., Huxel N., Meise H., von Neumann-Cosel P., Nicolay N., Pietralla N., H. Prade, J. Reif, A. Richter, C. Schlegel, R. Schwengner, S. Skoda, H. G. Thomas, I. Wiedenhöver, G. Winter, Zilges A. (1996). First observation of the scissors mode in a γ-soft nucleus: The Case of, Physical Review Letters, 76, 2029.

Von Brentano, P., Eberth, J., Enders, J., Esser, L., Herzberg, R.D., Huxel, N. & Zilges, A. (1996). First observation of the scissors mode in a γ-soft nucleus: The case of ^{196}Pt. *Physical Review Letters*, *76*(12), 2029.

Von Garrel, H., Brentano, P.V., Fransen, C., Friessner, G., Hollmann, N., Jolie, J. & Wisshak, K. (2006). Low-lying E1, M1 and E2 strength distributions in ^{124,126,128,129,130,131,132,134,136}Xe: Systematic photon scattering experiments in the mass region of a nuclear shape or phase transition. *Physical Review C-Nuclear Physics*, *73*(5), 054315.

Zenginerler, Z., Guliyev, E., Kuliev, A.A., Yakut, H. & Soluk, G. (2013). Systematic investigation of the low-lying dipole excitations in even-even $^{124-136}$Ba isotopes. *The European Physical Journal A, 49*(9), 107.